Phytopathology Research

RESEARCH

Open Access

The histone deacetylase HOS2 controls pathogenicity through regulation of melanin biosynthesis and appressorium formation in *Colletotrichum gloeosporioides*

Shike Liu[1†], Qiannan Wang[1,2†], Na Liu[1,2], Hongli Luo[1,2], Chaozu He[1,2] and Bang An[1,2*]

Abstract

The reversible acetylation of histones is effective for controlling chromatin dynamics and plays crucial roles in eukaryotes. In the present study, we identified and characterized a histone deacetylase HOS2 ortholog, designated CgHOS2, in *Colletotrichum gloeosporioides*. Knocking out *CgHOS2* resulted in decreased vegetative growth, impaired conidiation, and reduced stress tolerance. Moreover, the Δ*CgHOS2* mutant failed to form appressoria and lost pathogenicity on intact plant leaves. Western blot analysis revealed that CgHOS2 is responsible for the deacetylation of histone H3. Via transcriptomic analysis, a series of candidate genes controlled by CgHOS2 were predicted. Of these candidate genes, the expression of melanin biosynthesis-related enzymes was significantly reduced in vegetative hyphae and especially in appressoria, which led to a decrease in melanin content and failure of appressorium formation. Taken together, these results highlight the role of CgHOS2 in pathogenicity via regulation of melanin biosynthesis in *C. gloeosporioides*.

Keywords: Histone deacetylase HOS2, *Colletotrichum gloeosporioides*, Pathogenicity, Melanin, Appressorium

Background

The genus *Colletotrichum*, which comprises approximately 600 species, can infect more than 3200 plant species worldwide (O'Connell et al. 2012). Of these species, *Colletotrichum gloeosporioides* is a widespread pathogen that causes anthracnose disease on more than 470 plant species during the growing season and the postharvest stage (Phoulivong et al. 2010). Most *Colletotrichum* species employ a hemibiotrophic and multistage strategy during their infection life cycle, which includes conidial germination, dome-shaped appressorium formation, and production of biotrophic intracellular hyphae to infect living plant epidermal cells and necrotrophic hyphae that kill and destroy host tissues (O'Connell et al. 2012). Genome-wide expression profiling of three *Colletotrichum* species (*C. higginsianum*, *C. orbiculare*, and *C. gloeosporioides*) revealed that these hemibiotrophic pathogens affect the expression of virulence genes in a strict and successive pattern during the infection process (O'Connell et al. 2012; Gan et al. 2013).

In addition to transcription factors and distinct regulatory sequences in gene promoters, chromatin dynamics play an important role in the regulation of transcription in eukaryotes. Posttranslational modifications of histones, such as methylation, acetylation, phosphorylation, ubiquitylation, and sumoylation, have substantial

†Shike Liu and Qiannan Wang contributed equally to this work.

*Correspondence: anbang@hainanu.edu.cn

[1] Hainan Key Laboratory for Sustainable Utilization of Tropical Bioresource, Key Laboratory of Biotechnology of Salt Tolerant Crops of Hainan Province, College of Tropical Crops, Hainan University, Haikou 570228, Hainan, People's Republic of China
Full list of author information is available at the end of the article

structural consequences for chromatin architecture and thus play crucial roles in multiple biological processes (Bhaumik et al. 2007; Bird et al. 2007). The reversible acetylation of N-terminal core histone tails is controlled by two types of histone modification-related enzymes with opposing activities: histone acetyltransferases (HATs) and histone deacetylases (HDACs) (Vogelauer et al. 2000). HATs acetylate histones, physically relax chromatin, and thus activate gene expression, while HDACs remove acetyl groups from histones, which leads to a relatively condensed chromatin conformation and therefore repressing gene transcription. However, previous research has revealed that deacetylation of histones can also contribute to transcriptional activation (Verdin and Ott 2015). HDACs belong to a supergene family whose members widely exist in eukaryotes. Yeast HDACs are divided into three classes: Rpd3, HDA1, and SIR2 families (Kurdistani and Grunstein 2003). In vertebrates, four families of HDACs have been identified, namely, Rpd3s, HDA1s, SIR2s, and HDAC11s, which are different from those in yeast (Yang and Seto 2008). Plants have a unique HD2 family in addition to the typical RPD3, HDA1, and SIR2 HDAC families (Lusser et al. 2001).

In recent decades, histone deacetylation of fungal pathogens has attracted extensive amounts of attention because this process is associated with virulence traits and pathogenesis. In *Candida albicans*, the HDAC Set3/Hos2 complex regulates the morphological switch in yeast to produce pathogenic filamentous hyphae and is involved in resistance to fungicides (Hnisz et al. 2010; Li et al. 2017). The HDAC protein RpdA participates in hyphal growth in *Aspergillus nidulans* (Tribus et al. 2010). In the phytopathogenic fungi *Cochliobolus carbonum* and *Magnaporthe oryzae*, HOS2 proteins are required for pathogenicity because they are involved in regulating the invasion processes (Baidyaroy et al. 2001; Ding et al. 2010). In addition, HDACs are involved in toxin biosynthesis in phytopathogenic fungi, such as gibberellin biosynthesis in *Fusarium fujikuroi* (Studt et al. 2013), deoxynivalenol (DON) biosynthesis in *Fusarium graminearum* (Li et al. 2011), and aflatoxin biosynthesis in *Aspergillus flavus* and *Aspergillus niger* (Lan et al. 2019; Li et al. 2019). The HDAC Hos2 is required for the dimorphic switch and pathogenic development of *Ustilago maydis* (Elías-Villalobos et al. 2015).

However, the function of HDACs in the pathogenic life cycle of *C. gloeosporioides* is still unknown, and the potential targets of HDACs remain poorly characterized. Here, we identified a yeast HDA1 ortholog, CgHOS2, in *C. gloeosporioides* and investigated its roles in vegetative growth, conidiation, pathogenicity, and stress tolerance. In addition, via transcriptome analysis, we identified the possible target genes that are under the control of CgHOS2 and found that CgHOS2 is required for melanin biosynthesis and appressorium formation. Overall, our results provide new insights into the role of HDACs in fungal pathogenicity.

Results

Identification and bioinformatic analysis of CgHOS2

The HDAC protein-coding gene *CgHOS2* was identified through a BLASTP search of the *C. gloeosporioides* genome database, in which the *Saccharomyces cerevisiae* HDAC HOS2 (accession: ONH79409.1) protein sequence was used as a query. *CgHOS2* is predicted to contain a 1482-bp open reading frame without an intron and encodes a 494-aa protein (Additional file 1: Table S1), which shares 47.6% identity with *S. cerevisiae* HOS2. The protein domains were characterized using the Pfam database. The results showed that CgHOS2 contains a typical histone deacetylase domain at residues 81–382 (Fig. 1a). Phylogenetic analysis revealed that CgHOS2 and its orthologs from different plant pathogenic fungi are evolutionarily conserved (Fig. 1b).

CgHOS2 is localized to the nucleus

A CgHOS2-sGFP expression strain was constructed to investigate the subcellular localization of CgHOS2. The expression of *CgHOS2-sGFP* was driven by the promoter of the glyceraldehyde-3-phosphate dehydrogenase gene from *A. nidulans* (*PgpdA*) (Additional file 2: Figure S1), and a strain expressing an empty sGFP vector was used as a control. Observations with a confocal laser scanning microscope revealed that sGFP fluorescence was distributed in both the nucleus and the cytoplasm, whereas CgHOS2-sGFP-associated fluorescence was mainly located in the nucleus and colocalized with that of 4',6-diamidino-2-phenylindole (DAPI) (Fig. 2). Taken together, these results revealed that CgHOS2 is a nuclear protein.

Generation of the *CgHOS2* knockout mutant and complementation strains

To investigate the role of CgHOS2, the *CgHOS2* knockout mutant Δ*CgHOS2* was generated via a homologous recombination strategy (Additional file 2: Figure S2a). After protoplast transformation, the putative transformants were screened via two independent PCR analyses, and the results revealed that the recombination event occurred at the correct locus (Additional file 2: Figure S2b). Then, three independent Δ*CgHOS2* mutant strains were selected for subsequent analysis, and homozygotes of the corresponding transformants were purified via single-conidiospore isolation. The failure to amplify the target gene *CgHOS2* confirmed that this gene was completely knocked out of the genomes of the transformants.

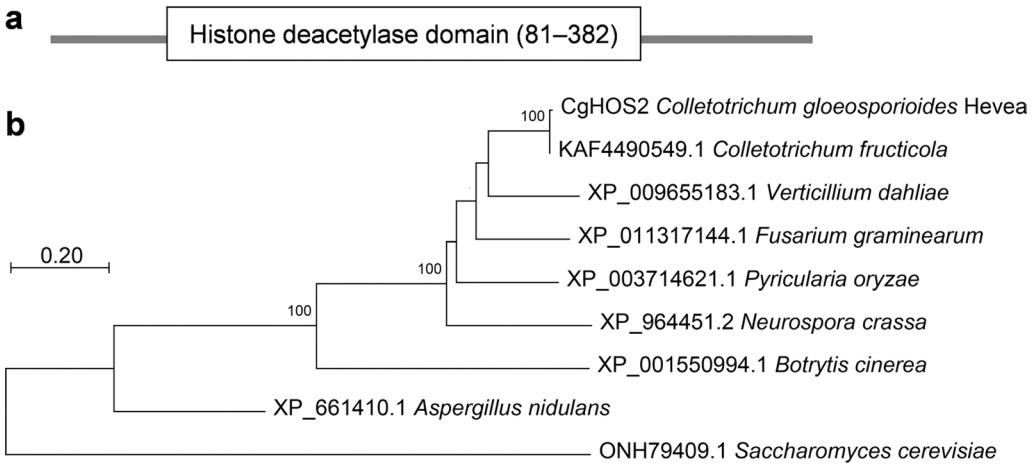

Fig. 1 Domain prediction and phylogenetic analysis of CgHOS2. **a** Domain prediction of CgHOS2. The histone deacetylase domain is indicated by a rectangle. **b** Phylogenetic relationship of CgHOS2 and its orthologs from several other fungal species. The HOS2 amino acid sequences were retrieved from the NCBI database, and the maximum likelihood phylogenetic tree was constructed using MEGA 11. The values in the tree indicate bootstrap values

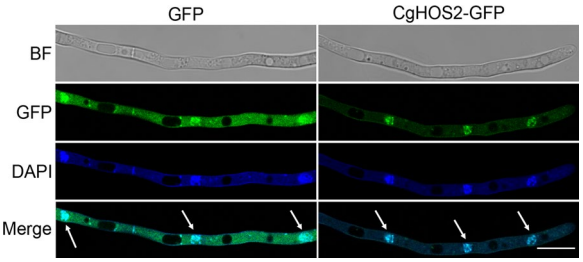

Fig. 2 Subcellular localization of CgHOS2. Fungal hyphae were visualized by confocal laser scanning fluorescence microscopy. The arrows indicate nuclei. BF, bright field. DAPI, 4′,6-diamidino-2-phenylindole. Scale bar = 10 μm

In addition, quantitative real-time PCR (qPCR) analysis results revealed that the three mutants contained a single copy of the acetolactate synthase gene (*SUR*) (Additional file 2: Figure S2c), suggesting that the homologous fragments were exclusively inserted at the *CgHOS2* locus. Moreover, a complementation strain Res-Δ*CgHOS2* was obtained by introduction of the *CgHOS2* expression cassette into the genome of Δ*CgHOS2* (Additional file 2: Figure S1).

CgHOS2 is involved in vegetative growth and conidiation

To investigate the role of CgHOS2 in vegetative growth, the growth rate of *C. gloeosporioides* strains on PDA media was determined. Δ*CgHOS2* showed a significant reduction in colony growth rate compared with those of the WT and Res-Δ*CgHOS2*, with the colony diameter decreasing by approximately 30% and 19% at 3 and 5 days post-inoculation (dpi), respectively (Fig. 3a, b). In addition, melanin biosynthesis in Δ*CgHOS2* was also obviously impaired in comparison with that in the WT and Res-Δ*CgHOS2* (Fig. 3a). Compared with that of the WT and Res-Δ*CgHOS2*, the conidiation of Δ*CgHOS2* was drastically inhibited, with conidial production decreasing by approximately 75% (Fig. 3c). These results indicate that CgHOS2 plays important roles in vegetative growth and conidiation of *C. gloeosporioides*.

CgHOS2 is involved in stress tolerance

To investigate the role of CgHOS2 in stress tolerance, the growth rate of *C. gloeosporioides* strains on PDA media supplemented with different chemicals was assayed. The results showed that the colony growth of Δ*CgHOS2* was significantly inhibited by treatment with H_2O_2, NaCl, or Congo red after incubation for 5 days, suggesting a reduced stress tolerance of Δ*CgHOS2* compared with the WT and Res-Δ*CgHOS2* (Fig. 4). Notably, 50 mmol/L H_2O_2 completely inhibited the growth of Δ*CgHOS2*, suggesting that CgHOS2 plays an important role in oxidative tolerance.

CgHOS2 is required for pathogenicity

To analyze the role of CgHOS2 in the pathogenicity of *C. gloeosporioides*, we conducted infection tests on rubber tree leaves. Intact leaves or pre-wounded leaves were inoculated with *C. gloeosporioides* to monitor the early penetration and late development processes of the pathogen. When they were inoculated on intact leaves, both the WT and Res-Δ*CgHOS2* caused obvious disease symptoms at 2 dpi and significant lesions at 4 dpi.

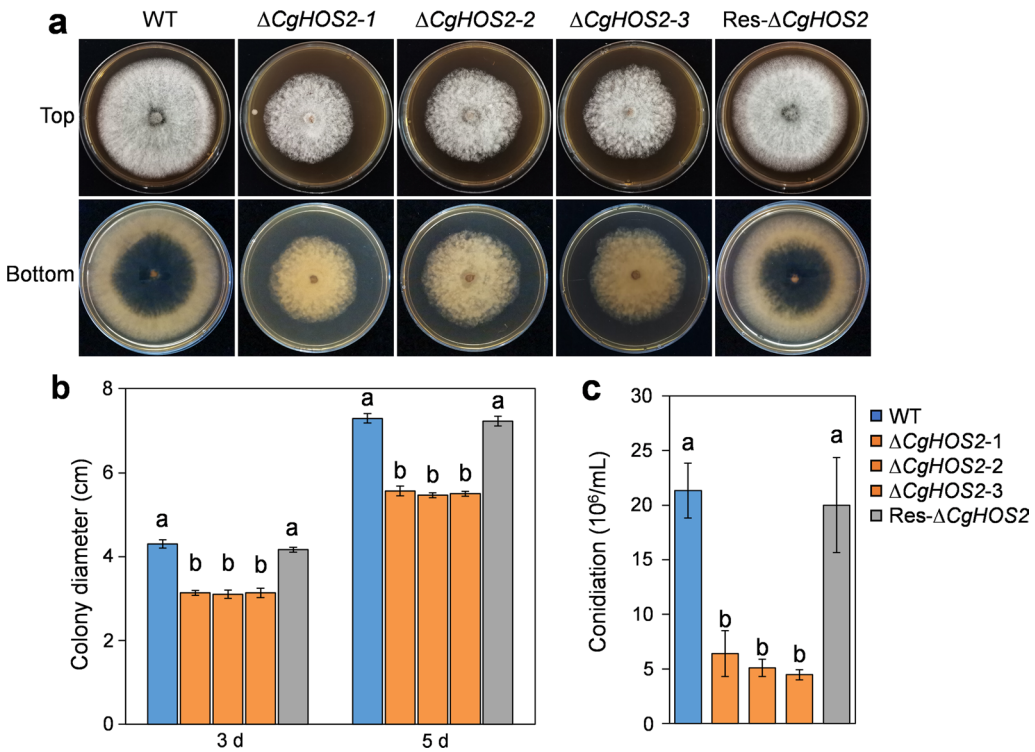

Fig. 3 CgHOS2 is involved in vegetative growth and conidiation. **a** Colony morphology of the WT, the *CgHOS2* knockout mutant Δ*CgHOS2*, and the complementation strain Res-Δ*CgHOS2* cultured on PDA media for 6 days. **b** Diameters of colonies of fungi cultured on PDA media for 3 and 5 days. **c** Conidiation after the fungi were incubated in PDA broth for 4 days. The values were analyzed with Duncan's multiple range tests. The columns with different letters indicate significant differences ($P < 0.05$)

In comparison, Δ*CgHOS2* nearly lost the ability to infect intact leaves, with disease incidences of 0%, 0%, and 1.67% at 2, 3, and 4 dpi, respectively (Fig. 5a and Table 1). When inoculated directly onto wounds of leaves, all the strains infected the leaves, with a disease incidence of 100%, but the lesions caused by Δ*CgHOS2* were significantly smaller than those caused by WT and Res-Δ*CgHOS2* (Fig. 5b and Table 1). These results suggested that CgHOS2 is essential for the pathogenicity of *C. gloeosporioides*, especially at the initial penetration stage.

CgHOS2 is required for appressorium formation and penetration ability

Conidial germination and appressorium formation of *C. gloeosporioides* were analyzed via incubation of conidia on both polyester and onion epidermal cells. When resuspended in ddH_2O, more than 80% of the conidia of the WT and Res-Δ*CgHOS2* germinated after incubation on polyester for 10 h, and approximately 50% of the conidia formed typical melanized appressoria. In comparison, only approximately 20% of conidia of Δ*CgHOS2* germinated, and 4% of conidia formed appressoria with abnormal shapes. Moreover, although most of the Δ*CgHOS2* conidia germinated after incubation for 20 h, they merely formed abnormally shaped appressoria and relatively longer germ tubes compared with those of WT and Res-Δ*CgHOS2* (Fig. 6a, c). When inoculated on onion epidermis, most of the conidia of the WT and Res-Δ*CgHOS2* germinated and formed typical appressoria at 6 h post-inoculation (hpi); in addition, the appressoria started to form invasive hyphae (also named primary hyphae) at 8 hpi. For Δ*CgHOS2*, more than 50% of the conidia germinated at 6 hpi, but there was no appressorium formation at 8 hpi (Fig. 6b, d). The penetration ability was also assayed by incubating the strains on cellophane. The results showed that Δ*CgHOS2* germinated normally on cellophane overlaid on nutrient-rich media (PDA) (Fig. 6f, g); however, after removal of the Δ*CgHOS2* colony together with the cellophane membrane and incubation for another 3 days, there were no colonies observed on the PDA media, suggesting that Δ*CgHOS2* lost its penetration ability and failed to grow into the media covered by cellophane. In comparison, the WT and Res-Δ*CgHOS2* successfully penetrated cellophane and grew into PDA media (Fig. 6e). Taken together, these results suggested that CgHOS2 is essential for the normal appressorium formation and penetration of *C. gloeosporioides*.

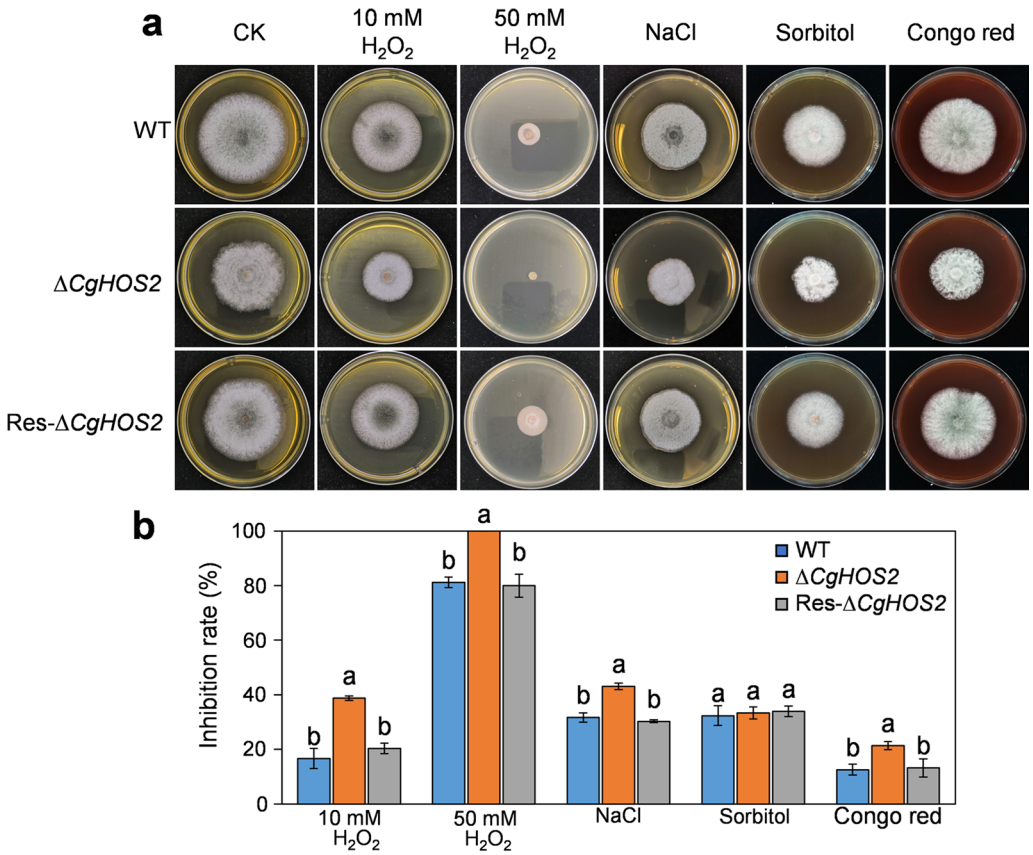

Fig. 4 CgHOS2 is involved in stress tolerance. **a** Colony morphology of fungi incubated on PDA media supplemented with 10 or 50 mmol/L H_2O_2, 0.7 mol/L NaCl, 1 mol/L sorbitol, or 0.25 mg/L Congo red for 6 days. **b** Column chart showing the inhibition rate of the tested chemicals. Strains cultured under nonstress conditions were used as controls. The inhibition rate was calculated with the following formula: Inhibition ratio (%) = (Area of control sample − Area of the treated sample)/(Area of control sample) × 100. The values were analyzed with Duncan's multiple range tests. The columns with different letters indicate significant differences ($P < 0.05$)

CgHOS2 is responsible for the deacetylation of histone H3

To explore whether CgHOS2 affects the acetylation status of H3, the same amount of total histones from the WT and Δ*CgHOS2* was subjected to western blot analysis. Anti-acetyl H3K9antibodies were used to estimate the acetylation status. The results showed that acetylation of H3 was obviously increased in Δ*CgHOS2* compared with the WT (Additional file 2: Figure S3), demonstrating that CgHOS2 is responsible for the deacetylation of histone H3.

Candidate genes regulated by CgHOS2

The transcriptomes of the WT and Δ*CgHOS2* were analyzed to explore the potential targets regulated by CgHOS2. The results showed that 4095 genes were differentially expressed (according to the criteria of $\log_2$FoldChange(FPKM + 2) > 1 ($\log_2$FC) and padj < 0.05) in Δ*CgHOS2* compared with the WT,of which 2286 were reduced and 1809 were increased in the transcript levels (Fig. 7a and Additional file 1: Table S2). Subsequent Gene Ontology (GO) enrichment analysis revealed that these genes were enriched in protein biosynthesis and metabolic processes, organic acid metabolic processes, and organonitrogen compound biosynthesis (Fig. 7b). Among these genes, transcripts of 102 of 108 major facilitator superfamily (MFS) proteins, 10 of 19 ATP-binding cassette (ABC) transporters, and 42 of 62 cell biosynthesis enzyme-coding genes were significantly reduced in Δ*CgHOS2* (Additional file 2: Figure S4), suggesting that CgHOS2 is involved in stress tolerance.

CgHOS2 regulates melanin biosynthesis

As observed in the growth assay (Fig. 3a), melanin biosynthesis of Δ*CgHOS2* was significantly impaired. As such, the melanin content of the *C. gloeosporioides* strains was measured after incubation in potato broth for 3 days. The results showed that the WT and Res-Δ*CgHOS2* produced 0.58 and 0.56 μg melanin/mg fresh mycelia, respectively, whereas Δ*CgHOS2* produced only 0.22 μg melanin/mg fresh mycelia (Fig. 8a). Seven enzymes and

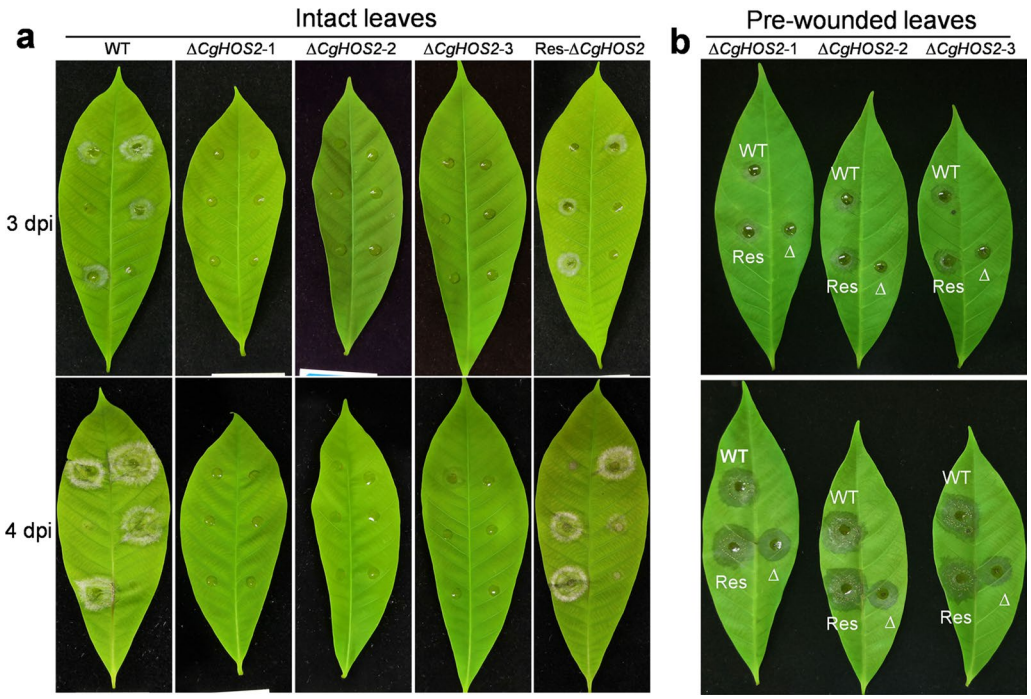

Fig. 5 CgHOS2 is required for the pathogenicity of *C. gloeosporioides*. **a** Symptoms on nonwounded rubber tree leaves at 3 and 4 dpi. **b** Symptoms on pre-wounded leaves at 3 and 4 dpi

Table 1 Disease incidence and severity caused by *C. gloeosporioides* on rubber tree leaves

Strain	Intact leaves		Pre-wounded leaves	
	Disease incidence (%)	Lesion diameter (mm)	Disease incidence (%)	Lesion diameter (mm)
WT	74.44 ± 2.55 a	9.52 ± 0.13 a	100	10.13 ± 0.24 a
Δ*CgHOS2*-1	0 b	0 b	100	4.87 ± 0.33 b
Δ*CgHOS2*-2	0 b	0 b	100	4.85 ± 0.26 b
Δ*CgHOS2*-3	0 b	0 b	100	4.84 ± 0.31 b
Res-Δ*CgHOS2*	73.89 ± 5.85 a	9.41 ± 0.15 a	100	9.80 ± 0.20 a

The values obtained at 3 days post-inoculation (dpi) were analyzed with Duncan's multiple range tests, and the different letters indicate significant differences ($P < 0.05$). The values are shown as the means ± standard deviations (SD) of three groups of samples

a transcription factor have been recognized as controlling melanin biosynthesis in plant pathogenic fungi: polyketide synthase (PKS), polyketide shortening (YG), HN reductase (T4HRa and T4HRb), scytalone dehydratase (SCD), multicopper oxidase (T3HR), laccase (LAC), and the transcription factor CMR1 (Tsai et al. 1999; Cho et al. 2012). Transcriptomics analysis revealed that the transcripts of all these 8 genes were reduced in Δ*CgHOS2* compared with the WT (Fig. 8b and Additional file 1: Table S2). Then, the transcriptomic data were verified via reverse transcription-quantitative PCR (RT-qPCR). The results showed that the expression levels of these genes were all reduced in Δ*CgHOS2*. Moreover, the expression of *CMR1*, *PKS*, *YG*, *T3HR*, and *LAC* was significantly upregulated in appressoria compared with that in hyphae in the WT (more than twofold, Fig. 8c), indicating their involvement in increased melanin biosynthesis in appressoria. Taken together, these results suggested that CgHOS2 plays an important role in melanin biosynthesis, especially at the appressorium formation stage, in *C. gloeosporioides*.

Discussion

Successive expression of virulence factors, including effectors, secondary metabolites, and plant-degrading enzymes, is critical for hemibiotrophic fungi such as *Colletotrichum* spp. to be able to infect hosts and complete their invasion life cycles (O'Connell et al. 2012;

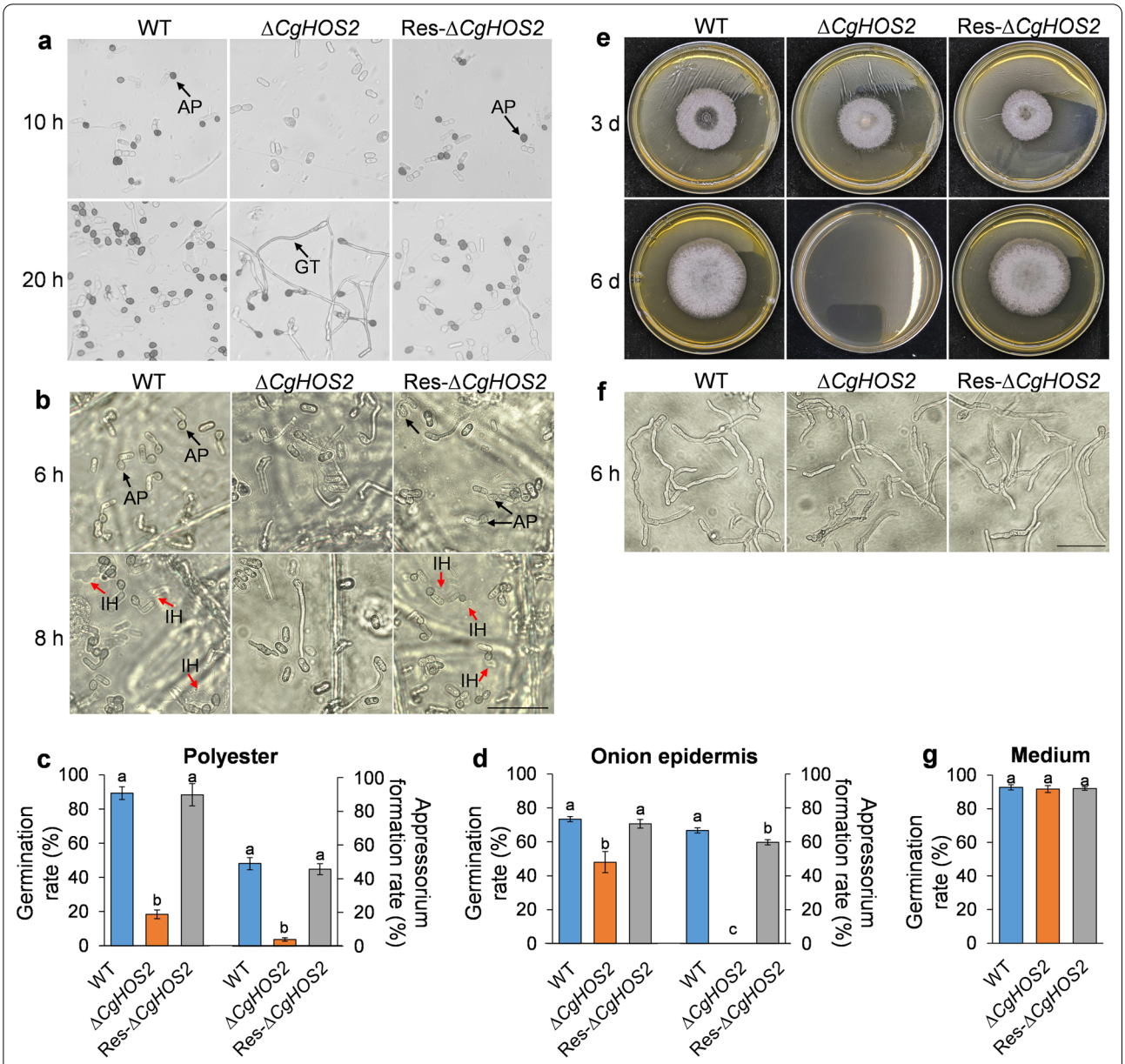

Fig. 6 CgHOS2 is required for normal appressorium formation and penetration. **a** Microscopy observations of conidia incubated on polyester for 10 and 20 h. The black arrows indicate appressoria (AP) and germ tubes (GT). Bar = 50 μm. **b** Microscopy observations of conidia incubated on onion epidermis for 6 and 8 h. The red arrows indicate invasive hyphae (IH). **c** Conidial germination and appressorium formation rates on polyester. **d** Conidial germination and appressorium formation rates on onion epidermis. **e** Colony morphology of fungi cultured on cellophane for 3 and 6 days. The cellophane membrane was removed after incubation for 3 days, followed by incubation for another 3 days. **f** Microscopy observations of conidia incubated on cellophane for 6 h. **g** Conidial germination rates on cellophane for 6 h. The values are shown as the means ± standard deviations (SD) of three groups of samples. The columns with different letters indicate significant differences ($P < 0.05$)

Soanes et al. 2012). Chromatin dynamics have a strong impact on transcriptional regulation (Steinfeld et al. 2007), and in fungal pathogens, histone acetylation and deacetylation are effective in regulating chromatin dynamics and play crucial roles in fungal development and pathogenicity (Shwab et al. 2007; González-Prieto et al. 2014; Elías-Villalobos et al. 2015; Liu et al. 2022). To investigate the biological roles of HDACs in *C. gloeosporioides*, the HDAC gene *CgHOS2*, encoding the ortholog of *S. cerevisiae* HOS2, was phylogenetically characterized and knocked out of the genome of the pathogen. Microscopy observations showed that CgHOS2-sGFP

Fig. 7 Transcriptome analysis of differentially expressed genes in Δ*CgHOS2* and the WT. **a** Scatter plots showing the genes that are differentially expressed in Δ*CgHOS2* and the WT (log_2FC(FPKM + 2) > 1 and FDR < 0.05). **b** GO enrichment analysis results of the differentially expressed genes

was mainly distributed in the nucleus, suggesting that CgHOS2 is a typical HDAC protein.

Knockout of *CgHOS2* in *C. gloeosporioides* cultured in vitro resulted in severe growth defects and a reduction in conidiation. Similar results were also observed for HDAC knockout mutants of *A. nidulans*, *U. maydis*, *M. oryzae*, *F. fujikuroi*, and *F. graminearum* (Reichmann et al. 2002; Ding et al. 2010; Tribus et al. 2010; Li et al. 2011; Studt et al. 2013). Transcriptomic analysis showed that 4095 genes were differentially expressed in Δ*CgHOS2*, of which a series of genes were enriched in protein biosynthesis. The results suggested that CgHOS2 might participate in vegetative growth and conidiation by regulating protein metabolism in *C. gloeosporioides*.

Previous research showed that HOS2 proteins are required for full virulence of pathogenic fungi such as *C. carbonum*, *M. oryzae*, and *F. graminearum* (Baidyaroy et al. 2001; Li et al. 2011; Studt et al. 2013). Our results revealed that CgHOS2 is also required for pathogenicity and especially for the early invasion of *C. gloeosporioides*. When inoculated onto leaf wounds, Δ*CgHOS2* could infect rubber tree leaves, and produced typical anthracnose symptoms, although it caused smaller lesions than the WT did, which might be due to the reduced growth rate of the mutant. However, when inoculated onto intact leaves, Δ*CgHOS2* caused almost no lesions at all, suggesting that the mutant lost the ability to infect its host. Since morphological changes and the formation of appressoria are critical for the infection of hemibiotrophic fungi in their hosts (Oh et al. 2008; O'Connell et al. 2012), we studied the germination behavior of *C. gloeosporioides* on both polyester and onion epidermis. Δ*CgHOS2* could not form typical appressoria on the polyester or onion epidermis during a short-term incubation, and only a small portion of conidia formed abnormally shaped appressoria, after incubation for 20 h on polyester. In comparison, the WT formed appressoria immediately after conidial germination on both the polyester and onion epidermis. Moreover, the penetration ability into cellophane was completely abolished in Δ*CgHOS2*. Taken together, these results suggested that CgHOS2 regulates pathogenicity by controlling appressorium formation in *C. gloeosporioides*. Similarly, HOS2 proteins are also required for appressorium formation, penetration, and post-penetration development in *M. oryzae*, *C. carbonum*, and *F. graminearum* (Baidyaroy et al. 2001; Izawa et al. 2009; Li et al. 2011; Studt et al. 2013).

Appressorium formation involves multiple signaling pathways, including those involved in MAP kinases, cAMP, the cell cycle, and autophagy (Xu and Hamer

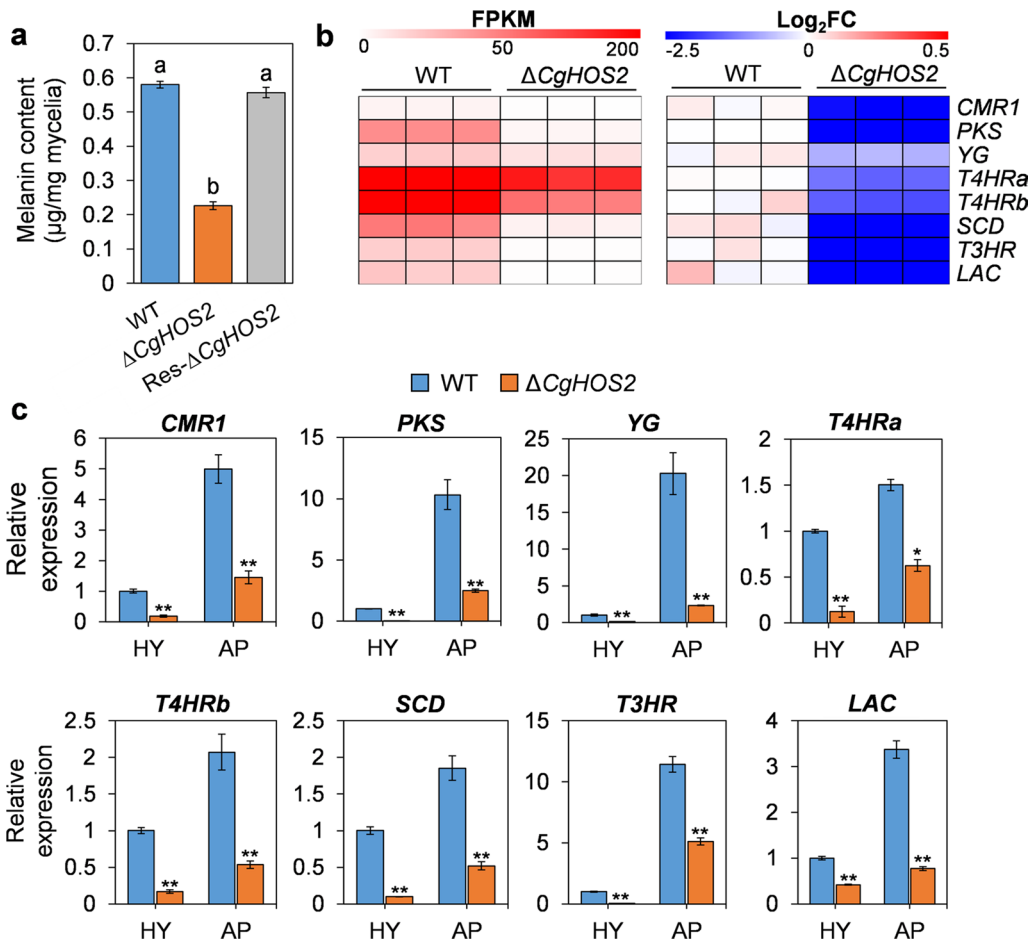

Fig. 8 CgHOS2 is required for melanin biosynthesis. **a** Measurement of melanin content in mycelia after incubation in potato broth for 3 days. **b** Relative transcript levels of 7 melanin biosynthesis-related enzymes and the transcription factor CMR1. The transcripts were expressed as FPKM values based on the transcriptomic data. FPKM + 2 normalized values were used to calculate the fold change (FC), and the relative levels were expressed as $\log_2$FC values. **c** Relative expression levels of the genes based on the RT-qPCR data; *β2-tubulin* was used as an endogenous control for normalization. The values are shown as the means ± standard deviations (SD). The columns with different letters indicate significant differences ($P < 0.05$), and the asterisks indicate significant differences at $P < 0.05$ (*) and $P < 0.01$ (**)

1996; Veneault-Fourrey et al. 2006; Saunders et al. 2010; Soanes et al. 2012); appressorium formation starts with the deposition of melanin in the cell wall, followed by the accumulation of glycerin and an increase in turgor pressure. Melanin deposition is required for turgor pressure generation and/or cell wall rigidity in appressoria (Money and Howard 1996; Ludwig et al. 2014). In *M. oryzae*, the deletion of *Mohda1*, an ortholog of yeast *hda1*, led to a significantly increased production of dark pigments in liquid culture (Maeda et al. 2017). Interestingly, here, we found that melanin biosynthesis was significantly reduced in Δ*CgHOS2* when cultured on PDA media, and the melanin content in Δ*CgHOS2* was reduced by nearly 66% compared with that in the WT. Most plant pathogenic fungi synthesize melanin via a so-called DHN pathway, which comprises 7 enzymes (Eisenman and Casadevall 2012; Pal et al. 2014). The coding genes of these 7 enzymes are usually physically linked in a cluster in the genomes of fungi (Slot and Rokas 2011), and the activation of these genes requires several specific transcription factors, such as CMR1 and HSF1 (Tsuji et al. 2000; Cho et al. 2012; Gao et al. 2022). The effects of CgHOS2 on the transcription of these 7 enzymes and CMR1 were investigated in this study. Based on the transcriptomic data and RT-qPCR verification results, the transcript levels of all 8 genes were reduced in Δ*CgHOS2*. Moreover, the expression levels of these genes were all significantly upregulated in the appressoria compared with those in the vegetative hyphae, and knockout of *CgHOS2* significantly

decreased the expression of these genes. These results suggested that CgHOS2 is critical for the activation of melanin biosynthesis and thus appressorium formation in *C. gloeosporioides*.

In addition to its specific roles in appressorium development, melanin is well known for its biological function in the detoxification of ROS and protection against environmental stresses in living cells. Therefore, we further tested the roles of CgHOS2 in stress tolerance. The results revealed that the tolerance of Δ*CgHOS2* to oxidative, salt, and cell wall inhibitor stress was decreased compared with that of the WT. In addition, the expression levels of a series of MFS and ABC transporters, which are related to stress tolerance (Reddy et al. 2012; Liu et al. 2021), were decreased in Δ*CgHOS2*, and the expression of many cell wall synthesis-related enzymes was also decreased in the mutant. The decrease in the stress tolerance of Δ*CgHOS2* might partly result from the repression of these genes. A similar result was also observed in an *HOS2* knockout mutant of *Beauveria bassiana*, which exhibited an increased sensitivity to oxidative stress compared with that of the wild-type strain (Cai et al. 2018). Thus, the roles of HDACs in stress tolerance make them potential antifungal targets (Bauer et al. 2016).

Conclusions

In this study, we identified a histone deacetylase, CgHOS2, in *C. gloeosporioides*. Our results indicate that CgHOS2 plays important roles in the regulation of vegetative growth, conidiation, pathogenicity, and stress tolerance in *C. gloeosporioides*; moreover, CgHOS2 is required for melanin biosynthesis and appressorium formation, both of which are critical for the pathogenicity of this fungal pathogen. Overall, our results provide new insights into the role of HOS2 in fungal pathogenicity.

Methods

Fungal strains and plant material

C. gloeosporioides isolated from *Hevea brasiliensis* (BioSample: SAMN17266943, https://www.ncbi.nlm.nih.gov/biosample/17266943) was cultured on potato dextrose agar medium (PDA) at 28 °C and used as the wild-type (WT) strain. The *H. brasiliensis* cultivar Reyan 7-33-97 was cultured in a glass house and used for the pathogenicity assay.

Bioinformatic analysis

To identify the yeast HDA1 ortholog (CgHOS2) in *C. gloeosporioides*, the amino acid sequence of the *S. cerevisiae* HDAC protein HOS2 (accession: ONH79409.1) was used to search against the genome sequence of *C. gloeosporioides*. The conserved domains of CgHOS2 were identified by searching against the Pfam database. The sequences of HOS2 orthologs from other phytopathogenic fungi were retrieved from the NCBI GenBank database, and a maximum likelihood tree was constructed via 1000 bootstraps with MEGA 11 (Tamura et al. 2021).

Construction of *CgHOS2* knockout, complementation, and CgHOS2-sGFP expression strains

The *CgHOS2* nucleotide sequence was knocked out via a homologous recombination strategy (Additional file 2: Figure S2a) involving the use of an acetolactate synthase gene cassette (*SUR*) from *M. oryzae* as the selective marker, which provides resistance to chlorimuron ethyl (a sulfonylurea herbicide). The up- and down-stream flanking fragments of *CgHOS2* were ligated to *SUR* and used for protoplast transformation. For gene complementation, the full-length coding region of *CgHOS2* together with its native 1 kb promoter sequence was cloned into a plasmid containing the terminator of tryptophan synthase from *A. nidulans* (TtrpC) and the hygromycin phosphotransferase gene (*HPT*) (Additional file 2: Figure S1a). For the construction of the CgHOS2-sGFP expression strain, the coding sequence of *CgHOS2* was cloned into a modified pMD19-T plasmid, which contains an expression cassette including the *PgpdA* promoter, sGFP coding sequence, the terminator TtrpC, and *HPT* (Additional file 2: Figure S1a). The gene complementation and CgHOS2-sGFP expression plasmids were linearized before protoplast transformation. Protoplast preparation and transformation were carried out as described previously (Liu et al. 2021). At 3–4 days after transformation, the transformants resistant to chlorimuron ethyl or hygromycin B were selected for further PCR detection. For gene knockout mutants, two independent PCR assays were conducted with the primer pairs HOS2-DF/SUR-DR and SUR-DF/HOS2-DR, of which one primer targeted the regions up- or down-stream of the flanking fragments and the other primer targeted regions within *SUR* (Additional file 2: Figure S2a). After electrophoresis, the target DNA bands were sequenced. Then, the confirmed transformants were purified by single-conidiospore isolation, and the presence of *CgHOS2* was further checked via PCR. The copy numbers of the inserted fragments were analyzed via qPCR analysis, with *SUR* used as a probe and *β2-tubulin* used as an endogenous control. Confirmation of gene complementation and CgHOS2-sGFP was carried out by detection of *CgHOS2* and *CgHOS2-sGFP*, respectively (Additional file 2: Figure S1b). The primers used are listed in Additional file 1: Table S3.

Stress tolerance assay

For the stress tolerance assay, *C. gloeosporioides* strains were cultured on PDA media supplemented with 10 and 50 mmol/L H_2O_2, 0.7 mol/L NaCl, 1 mol/L sorbitol, and 0.25 mg/L Congo red to simulate oxidative, salt, osmotic, and fungal cell wall inhibitor stresses, respectively. Colony diameters were recorded after the strains were incubated for 5 days. The strain cultured without chemical treatment was used as a control, and the relative inhibition rate was calculated with the following formula: Inhibition ratio (%) = (Area of control sample − Area of the treated sample)/(Area of control sample) × 100. Each treatment involves three replicates, and all the experiments were performed twice.

Pathogenicity assay

The pathogenicity assay was performed as described previously (Gao et al. 2022). A *C. gloeosporioides* conidial suspension (2×10^5 conidia/mL) was drop-inoculated onto rubber tree leaves that were previously wounded or not wounded. The inoculated leaves were maintained in Petri dishes at 28 °C under natural illumination for 2–4 days before disease incidence and lesion diameter were recorded. Each treatment involved three replicates of 10 leaves, and the experiment was repeated three times.

Appressorium formation and penetration ability assay

Appressorium formation and subsequent invasion assays were conducted by incubating *C. gloeosporioides* conidia on both polyester and onion epidermis. Polyester with a thickness of 25 μm was placed on water agar; aliquots of conidial suspension were inoculated onto the polyester; and conidial germination and appressorium formation were observed under a microscope after incubation for 10 and 20 h. Onion epidermis was put on water agar plates and inoculated with the conidial suspension. After incubation for 6 and 8 h, the infection structures were observed. For microscopy observation, at least 50 conidia were counted. Each treatment contained three replicates, and the experiment was repeated two times.

The penetration ability of *C. gloeosporioides* was investigated by incubating the strains on PDA medium overlaid with a cellophane membrane. After *C. gloeosporioides* strains were cultured on the cellophane for 3 days, the cellophane was removed, the petri dishes were incubated for another 3 days, and the colony development on PDA media was observed.

Western blot analysis

First, conidia were inoculated into liquid potato broth (without dextrose) with an initial concentration of 10^3 conidia/mL and incubated for 2 days at 28 °C under 160 rpm. Then, mycelia were collected, ground to a powder in liquid nitrogen, and used for histone isolation with an EpiQuik Total Histone Extraction Kit (Epigentek, Farmingdale, NY, USA). Histone samples were electrophoresed on 15% polyacrylamide gels and blotted onto PVDF membranes. Immunological detection was performed using anti-histone H3 and anti-histone H3 (acetyl K9) antibodies (catalog numbers ab201456 and ab177177, respectively; Abcam, Cambridge, UK).

RNA-seq analysis

The mycelia were prepared as mentioned above, ground to powder in liquid nitrogen, and used for RNA isolation with an RNAprep Pure Plant Plus Kit (TIANGEN Biotech, Beijing, China). Library preparation and sequencing were conducted by staff at Novogene (Beijing, China) on an Illumina NovaSeq platform. Each group of samples involved three biological replicates, and at least 6 gigabytes (GB) of clean data were obtained for each replicate. The genome of *Colletotrichum fructicola* Nara gc5 (version: RPSC_Cfru_v1.0 [https://www.ncbi.nlm.nih.gov/assembly/GCF_000319635.1/]) was used as a reference genome. The DESeq2 R package was employed to analyze differential expression. Normalized FPKM + 2 values were used to calculate the gene expression level FCs, and the genes with $|\log_2 FC| > 1$ and adjusted *P* value (padj) < 0.05 were considered differentially expressed. The differentially expressed genes (DEGs) were further analyzed according to their Kyoto Encyclopedia of Genes and Genomes (KEGG) enrichment. The data were deposited in the NCBI database under BioProject PRJNA747883.

RT-qPCR analysis

Total RNA was isolated from the mycelia as described above. For isolation of RNA from appressoria, a conidial suspension at a concentration of 10^5 conidia/mL was plated onto polyester, which was placed on water agar. After incubation for 18 h, the appressoria were collected with a cell scraper and used for RNA isolation. First-strand cDNA was synthesized with FastKing gDNA Dispelling RT SuperMix (TIANGEN Biotech, Beijing, China), and qPCR analysis was performed with ChamQ SYBR Color qPCR Master Mix (Vazyme, Nanjing, China) using QuantStudio 6 (Thermo Fisher, Waltham, MA, USA). The relative transcript levels were estimated using the $2^{-\Delta\Delta Ct}$ method, with *β2-tubulin* used as an endogenous control and mycelia from the WT used as reference samples. Each reaction involved three biological replicates.

Measurement of melanin content

The melanin content was measured with a fungal melanin quantification kit (Genmed Scientific, Inc., USA). Briefly,

conidia were inoculated into potato broth media with an initial concentration of 10^3 conidia/mL and incubated for 3 days at 28 °C under 160 rpm. Then, mycelia were collected, ground to powder in liquid nitrogen, and used for melanin extraction. The melanin content was quantitated by measuring the absorbance at 360 nm using a spectrophotometer (Eppendorf, Germany). Both the WT and the mutant were biologically replicated three times.

Abbreviations

ABC: ATP-binding cassette; AP: Appressoria; DAPI: 4′,6-Diamidino-2-phenylindole; DEGs: Differentially expressed genes; DON: Deoxynivalenol; dpi: Days post-inoculation; FC: Fold change; FPKM: Fragments per kilobase of exon model per million mapped fragments; GB: Gigabyte; GFP: Green fluorescent protein; GO: Gene ontology; GT: Germ tube; HATs: Histone acetyltransferases; HDAC: Histone deacetylase; hpi: Hours post-inoculation; HPT: Hygromycin phosphotransferase gene; IH: Invasive hyphae; KEGG: Kyoto encyclopedia of genes and genomes; MFS: Major facilitator superfamily; PDA: Potato dextrose agar medium; qPCR: Quantitative real-time PCR; RT-qPCR: Reverse transcription-quantitative PCR; PgpdA: Promoter of the glyceraldehyde-3-phosphate dehydrogenase gene from *A. nidulans*; TtrpC: Terminator of tryptophan synthase of *A. nidulans*; WT: Wild type.

Supplementary Information

The online version contains supplementary material available at https://doi.org/10.1186/s42483-022-00126-0.

Additional file 1: **Table S1**. Nucleotide and deduced amino acid sequences of CgHOS2. **Table S2**. RNA-seq results. **Table S3**. Primers used in this study.

Additional file 2: **Figure S1**. Construction of the complementation strain and CgHOS2-sGFP expression strain. **Figure S2**. Construction of the *CgHOS2* knockout mutant. **Figure S3**. Histone acetylation status in Δ*CgHOS2*. **Figure S4**. Hierarchical clustering of the genes that are involved in stress tolerance based on RNA-seq data.

Acknowledgements

Not applicable.

Author contributions

SL and QW performed the experiment and wrote the manuscript. NL helped perform pathogenicity analysis. CH and HL revised the manuscript. BA designed the experiment and revised the manuscript. All authors read and approved the final manuscript.

Funding

This research was funded by the National Natural Science Foundation of China (32000102, 32160594, 32001846, 32060591).

Availability of data and materials

The datasets generated and analyzed during the current study are available in the NCBI repository [https://www.ncbi.nlm.nih.gov/bioproject/PRJNA747883].

Declarations

Ethics approval and consent to participate

Not applicable.

Consent for publication

Not applicable.

Competing interests

The authors declare that they have no competing interests.

Author details

[1]Hainan Key Laboratory for Sustainable Utilization of Tropical Bioresource, Key Laboratory of Biotechnology of Salt Tolerant Crops of Hainan Province, College of Tropical Crops, Hainan University, Haikou 570228, Hainan, People's Republic of China. [2]Sanya Nanfan Research Institute of Hainan University, Hainan Yazhou Bay Seed Laboratory, Sanya 572025, Hainan, People's Republic of China.

Received: 4 March 2022 Accepted: 16 May 2022
Published online: 06 June 2022

References

Baidyaroy D, Brosch G, Ahn JH, Graessle S, Wegener S, Tonukari NJ, et al. A gene related to yeast *HOS2* histone deacetylase affects extracellular depolymerase expression and virulence in a plant pathogenic fungus. Plant Cell. 2001;13(7):1609–24. https://doi.org/10.1105/tpc.010168.

Bauer I, Varadarajan D, Pidroni A, Gross S, Vergeiner S, Faber B, et al. A Class 1 histone deacetylase with potential as an antifungal target. mBio. 2016 1;7(6):e00831–16. https://doi.org/10.1128/mBio.00831-16.

Bhaumik SR, Smith E, Shilatifard A. Covalent modifications of histones during development and disease pathogenesis. Nat Struct Mol Biol. 2007;14(11):1008–16. https://doi.org/10.1038/nsmb1337.

Bird A. Perceptions of epigenetics. Nature. 2007;447(7143):396–8. https://doi.org/10.1038/nature05913.

Cai Q, Tong SM, Shao W, Ying SH, Feng MG. Pleiotropic effects of the histone deacetylase Hos2 linked to H4–K16 deacetylation, H3–K56 acetylation, and H2A–S129 phosphorylation in *Beauveria bassiana*. Cell Microbiol. 2018;20(7): e12839. https://doi.org/10.1111/cmi.12839.

Cho Y, Srivastava A, Ohm RA, Lawrence CB, Wang KH, Grigoriev IV, et al. Transcription factor Amr1 induces melanin biosynthesis and suppresses virulence in *Alternaria brassicicola*. PLoS Pathog. 2012;8(10): e1002974. https://doi.org/10.1371/journal.ppat.1002974.

Ding SL, Liu W, Iliuk A, Ribot C, Vallet J, Tao A, et al. The tig1 histone deacetylase complex regulates infectious growth in the rice blast fungus *Magnaporthe oryzae*. Plant Cell. 2010;22(7):2495–508. https://doi.org/10.1105/tpc.110.074302.

Eisenman HC, Casadevall A. Synthesis and assembly of fungal melanin. Appl Microbiol Biotechnol. 2012;93(3):931–40. https://doi.org/10.1007/s00253-011-3777-2.

Elías-Villalobos A, Fernández-Álvarez A, Moreno-Sánchez I, Helmlinger D, Ibeas JI. The Hos2 histone deacetylase controls *Ustilago maydis* virulence through direct regulation of mating-type genes. PLoS Pathog. 2015;11(8): e1005134. https://doi.org/10.1371/journal.ppat.1005134.

Gan P, Ikeda K, Irieda H, Narusaka M, O'Connell RJ, Narusaka Y, et al. Comparative genomic and transcriptomic analyses reveal the hemibiotrophic stage shift of *Colletotrichum* fungi. New Phytol. 2013;197(4):1236–49. https://doi.org/10.1111/nph.12085.

Gao X, Wang Q, Feng Q, Zhang B, He C, Luo H, et al. Heat shock transcription factor CgHSF1 is required for melanin biosynthesis, appressorium formation, and pathogenicity in *Colletotrichum gloeosporioides*. J Fungi (basel). 2022;8(2):175. https://doi.org/10.3390/jof8020175.

González-Prieto JM, Rosas-Quijano R, Domínguez A, Ruiz-Herrera J. The *UmGcn5* gene encoding histone acetyltransferase from *Ustilago maydis* is involved in dimorphism and virulence. Fungal Genet Biol. 2014;71:86–95. https://doi.org/10.1016/j.fgb.2014.09.002.

Hnisz D, Majer O, Frohner IE, Komnenovic V, Kuchler K. The Set3/Hos2 histone deacetylase complex attenuates cAMP/PKA signaling to regulate morphogenesis and virulence of *Candida albicans*. PLoS Pathog. 2010;6(5): e1000889. https://doi.org/10.1371/journal.ppat.1000889.

Izawa M, Takekawa O, Arie T, Teraoka T, Yoshida M, Kimura M, et al. Inhibition of histone deacetylase causes reduction of appressorium formation in the rice blast fungus *Magnaporthe oryzae*. J Gen Appl Microbiol. 2009;55(6):489–98. https://doi.org/10.2323/jgam.55.489.

Kurdistani SK, Grunstein M. Histone acetylation and deacetylation in yeast. Nat Rev Mol Cell Biol. 2003;4(4):276–84. https://doi.org/10.1038/nrm1075.

Lan H, Wu L, Sun R, Keller NP, Yang K, Ye L, et al. The HosA histone deacetylase regulates aflatoxin biosynthesis through direct regulation of aflatoxin cluster genes. Mol Plant Microbe Interact. 2019;32(9):1210–28. https://doi.org/10.1094/MPMI-01-19-0033-R.

Li X, Pan L, Wang B, Pan L. The histone deacetylases HosA and HdaA affect the phenotype and transcriptomic and metabolic profiles of *Aspergillus niger*. Toxins (basel). 2019;11(9):520. https://doi.org/10.3390/toxins11090520.
Li X, Robbins N, O'Meara TR, Cowen LE. Extensive functional redundancy in the regulation of *Candida albicans* drug resistance and morphogenesis by lysine deacetylases Hos2, Hda1, Rpd3 and Rpd31. Mol Microbiol. 2017;103(4):635–56. https://doi.org/10.1111/mmi.13578.
Li Y, Wang C, Liu W, Wang G, Kang Z, Kistler HC, et al. The *HDF1* histone deacetylase gene is important for conidiation, sexual reproduction, and pathogenesis in *Fusarium graminearum*. Mol Plant Microbe Interact. 2011;24(4):487–96. https://doi.org/10.1094/MPMI-10-10-0233.
Liu J, An B, Luo H, He C, Wang Q. The histone acetyltransferase FocGCN5 regulates growth, conidiation, and pathogenicity of the banana wilt disease causal agent *Fusarium oxysporum* f.sp. *cubense* tropical race 4. Res Microbiol. 2022; 173(3):103902. https://doi.org/10.1016/j.resmic.2021.103902.
Liu N, Wang Q, He C, An B. CgMFS1, a major facilitator superfamily transporter, is required for sugar transport, oxidative stress resistance, and pathogenicity of *Colletotrichum gloeosporioides* from *Hevea brasiliensis*. Curr Issues Mol Biol. 2021;43(3):1548–57. https://doi.org/10.3390/cimb43030109.
Ludwig N, Löhrer M, Hempel M, Mathea S, Schliebner I, Menzel M, et al. Melanin is not required for turgor generation but enhances cell-wall rigidity in appressoria of the corn pathogen *Colletotrichum graminicola*. Mol Plant Microbe Interact. 2014;27(4):315–27. https://doi.org/10.1094/MPMI-09-13-0267-R.
Lusser A, Kölle D, Loidl P. Histone acetylation: lessons from the plant kingdom. Trends Plant Sci. 2001;6(2):59–65. https://doi.org/10.1016/s1360-1385(00)01839-2.
Maeda K, Izawa M, Nakajima Y, Jin Q, Hirose T, Nakamura T, et al. Increased metabolite production by deletion of an HDA1-type histone deacetylase in the phytopathogenic fungi, *Magnaporthe oryzae* (*Pyricularia oryzae*) and *Fusarium asiaticum*. Lett Appl Microbiol. 2017;65(5):446–52. https://doi.org/10.1111/lam.12797.
Money NP, Howard RJ. Confirmation of a link between fungal pigmentation, turgor pressure, and pathogenicity using a new method of turgor measurement. Fungal Genet Biol. 1996;20:217–27.https://doi.org/10.1006/fgbi.1996.0037.
O'Connell RJ, Thon MR, Hacquard S, Amyotte SG, Kleemann J, Torres MF, et al. Lifestyle transitions in plant pathogenic *Colletotrichum* fungi deciphered by genome and transcriptome analyses. Nat Genet. 2012;44(9):1060–5. https://doi.org/10.1038/ng.2372.
Oh Y, Donofrio N, Pan H, Coughlan S, Brown DE, Meng S, et al. Transcriptome analysis reveals new insight into appressorium formation and function in the rice blast fungus *Magnaporthe oryzae*. Genome Biol. 2008;9(5):R85. https://doi.org/10.1186/gb-2008-9-5-r85.
Pal AK, Gajjar DU, Vasavada AR. DOPA and DHN pathway orchestrate melanin synthesis in *Aspergillus species*. Med Mycol. 2014;52(1):10–8. https://doi.org/10.3109/13693786.2013.826879.
Phoulivong S, Cai L, Chen H, McKenzie EH, Abdelsalam K, Chukeatirote E, et al. *Colletotrichum gloeosporioides* is not a common pathogen on tropical fruits. Fungal Divers. 2010;44:33–43. https://doi.org/10.1080/12298093.2018.1454010.
Reddy VS, Shlykov MA, Castillo R, Sun EI, Saier MH Jr. The major facilitator superfamily (MFS) revisited. FEBS J. 2012;279(11):2022–35. https://doi.org/10.1111/j.1742-4658.2012.08588.x.
Reichmann M, Jamnischek A, Weinzierl G, Ladendorf O, Huber S, Kahmann R, et al. The histone deacetylase Hda1 from *Ustilago maydis* is essential for teliospore development. Mol Microbiol. 2002;46(4):1169–82. https://doi.org/10.1046/j.1365-2958.2002.03238.x.
Saunders DG, Aves SJ, Talbot NJ. Cell cycle-mediated regulation of plant infection by the rice blast fungus. Plant Cell. 2010;22(2):497–507. https://doi.org/10.1105/tpc.109.072447.
Shwab EK, Bok JW, Tribus M, Galehr J, Graessle S, Keller NP. Histone deacetylase activity regulates chemical diversity in *Aspergillus*. Eukaryot Cell. 2007;6(9):1656–64. https://doi.org/10.1128/EC.00186-07.
Slot JC, Rokas A. Horizontal transfer of a large and highly toxic secondary metabolic gene cluster between fungi. Curr Biol. 2011;21(2):134–9. https://doi.org/10.1016/j.cub.2010.12.020.
Soanes DM, Chakrabarti A, Paszkiewicz KH, Dawe AL, Talbot NJ. Genome-wide transcriptional profiling of appressorium development by the rice blast fungus *Magnaporthe oryzae*. PLoS Pathog. 2012;8(2): e1002514. https://doi.org/10.1371/journal.ppat.1002514.
Steinfeld I, Shamir R, Kupiec M. A genome-wide analysis in *Saccharomyces cerevisiae* demonstrates the influence of chromatin modifiers on transcription. Nat Genet. 2007;39(3):303–9. https://doi.org/10.1038/ng1965.
Studt L, Schmidt FJ, Jahn L, Sieber CM, Connolly LR, Niehaus EM, et al. Two histone deacetylases, FfHda1 and FfHda2, are important for *Fusarium fujikuroi* secondary metabolism and virulence. Appl Environ Microbiol. 2013;79(24):7719–34. https://doi.org/10.1128/AEM.01557-13.
Tamura K, Stecher G, Kumar S. MEGA11: molecular evolutionary genetics analysis version 11. Mol Biol Evol. 2021;38(7):3022–7. https://doi.org/10.1093/molbev/msab120.
Tribus M, Bauer I, Galehr J, Rieser G, Trojer P, Brosch G, et al. A novel motif in fungal class 1 histone deacetylases is essential for growth and development of *Aspergillus*. Mol Biol Cell. 2010;21(2):345–53. https://doi.org/10.1091/mbc.e09-08-0750.
Tsai HF, Wheeler MH, Chang YC, Kwon-Chung KJ. A developmentally regulated gene cluster involved in conidial pigment biosynthesis in *Aspergillus fumigatus*. J Bacteriol. 1999;181(20):6469–77. https://doi.org/10.1128/jb.181.20.6469-6477.1999.
Tsuji G, Kenmochi Y, Takano Y, Sweigard J, Farrall L, Furusawa I, et al. Novel fungal transcriptional activators, Cmr1p of *Colletotrichum lagenarium* and pig1p of *Magnaporthe grisea*, contain Cys2His2 zinc finger and Zn(II)2Cys6 binuclear cluster DNA-binding motifs and regulate transcription of melanin biosynthesis genes in a developmentally specific manner. Mol Microbiol. 2000;38(5):940–54. https://doi.org/10.1046/j.1365-2958.2000.02181.x.
Veneault-Fourrey C, Barooah M, Egan M, Wakley G, Talbot NJ. Autophagic fungal cell death is necessary for infection by the rice blast fungus. Science. 2006;312(5773):580–3. https://doi.org/10.1126/science.1124550.
Verdin E, Ott M. 50 years of protein acetylation: from gene regulation to epigenetics, metabolism and beyond. Nat Rev Mol Cell Biol. 2015;16(4):258–64. https://doi.org/10.1038/nrm3931.
Vogelauer M, Wu J, Suka N, Grunstein M. Global histone acetylation and deacetylation in yeast. Nature. 2000;408(6811):495–8. https://doi.org/10.1038/35044127.
Xu JR, Hamer JE. MAP kinase and cAMP signaling regulate infection structure formation and pathogenic growth in the rice blast fungus *Magnaporthe grisea*. Genes Dev. 1996;10(21):2696–706. https://doi.org/10.1101/gad.10.21.2696.
Yang XJ, Seto E. The Rpd3/Hda1 family of lysine deacetylases: from bacteria and yeast to mice and men. Nat Rev Mol Cell Biol. 2008;9(3):206–18. https://doi.org/10.1038/nrm2346.

Publisher's Note